Phase Transitions
Publication details, including instructions for authors and subscription information:
http://www.tandfonline.com/loi/gpht20

Characterization of nanostructured ceramics prepared by both high energy ball milling and fast firing sintering processes

Y. Leyet [a], F. Guerrero [a b], E. Pérez-Delfín [a b], J. Pérez de la Cruz [c] & J.A. Eiras [b]

[a] Departamento de Física, Facultad de Ciencias Naturales, Universidad de Oriente, Santiago de Cuba C.P. 90500, Cuba

[b] Departamento de Física, Grupo de Cerâmicas Ferroelétricas, Universidade Federal de São Carlos (UFSCar), São Carlos/São Paulo CEP: 13565-670, Brazil

[c] INESCPorto, Rua do Campo Alegre, 687, Porto 4169-007, Portugal

Available online: 25 Jul 2011

To cite this article: Y. Leyet, F. Guerrero, E. Pérez-Delfín, J. Pérez de la Cruz & J.A. Eiras (2012): Characterization of nanostructured ceramics prepared by both high energy ball milling and fast firing sintering processes, Phase Transitions, 85:1-2, 136-148

To link to this article: http://dx.doi.org/10.1080/01411594.2011.596132

Phase Transitions
Vol. 85, Nos. 1–2, January–February 2012, 136–148

Characterization of nanostructured ceramics prepared by both high energy ball milling and fast firing sintering processes

Y. Leyet[a], F. Guerrero[ab], E. Pérez-Delfín[ab], J. Pérez de la Cruz[c*] and J.A. Eiras[b]

[a]*Departamento de Física, Facultad de Ciencias Naturales, Universidad de Oriente, Santiago de Cuba C.P. 90500, Cuba;* [b]*Departamento de Física, Grupo de Cerâmicas Ferroelétricas, Universidade Federal de São Carlos (UFSCar), São Carlos/São Paulo CEP: 13565-670, Brazil;* [c]*INESCPorto, Rua do Campo Alegre, 687, Porto 4169-007, Portugal*

(*Received 16 April 2011; final version received 8 June 2011*)

High-energy ball milling technique was successfully applied to calcinated lead zirconate titanate (PZT 60/40) powders. After 20 h of ball milling, large PZT particles were completely broken down, reducing its initial size in three orders of magnitude. Experimental results show a huge sinterability enhancement of the PZT powders by using this technique, achieving its maximum sintering rate at ~800°C. Relatively low densities (~91%) were achieved in stoichiometric samples, while in 3% lead excess samples sintered at 950°C for 30, 45, 60, 90 and 120 min using a fast firing process and a post-annealing treatment at 800°C for 4 h, densities of ~97% of the theoretical were achieved. PZT nanostructured ceramics prepared under optimized processing conditions (60 h of powder milling, 950°C of sintering temperature, 60 min of sintering time and a post-annealing process at 800°C during 4 h) show high dielectric constant (ε') values (900) and low dielectric loss ($\tan\delta$) at room temperature and a ferroelectric-paraelectric transition temperature at 375°C.

Keywords: high-energy ball milling; fast firing; PZT nanostructured ceramics; dielectric properties

1. Introduction

Piezoelectric lead zirconate titanate ceramics ($PbZr_{1-x}Ti_xO_3$ or simply PZT), with a perovskite structure, have been widely investigated for several electronic applications (i.e. transducers, ferroelectric memories, sonars, optical filters, shutters, actuators and modulators; [1–6]). Generally, PZT powders are prepared by a traditional method (solid-state reaction), which involves mixing of the precursor oxides (PbO, TiO_2 and ZrO_2) in stoichiometric ratio, calcination of the green powders at a relative low temperature and sintering at high temperatures [1]. However, due to its high volatility lead-containing piezoelectric materials show higher lead losses during their sintering at high temperatures, which result in poor electrical, optical and electromechanical properties. It is well-known that in order to avoid the lead losses during the sintering process it is necessary to reduce

*Corresponding author. Email: jcruz@inscporto.pt

ISSN 0141–1594 print/ISSN 1029–0338 online

http://dx.doi.org/10.1080/01411594.2011.596132
http://www.tandfonline.com

the sintering temperature, which could be archived with a small grain size and narrow size distribution of the precursor powders. For this purpose in the last few decades, submicron or even nanosize ferroelectric powders have been prepared by various wet-chemistry methods, including chemical co-precipitation [7,8], sol-gel process [9,10] and hydrothermal synthesis [11,12]. Although significant progresses have been achieved by these methods, their higher sensitivity to the environmental conditions (i.e. humidity, light and heat) and the high price of their precursor reagents, limit the applicability of these methods [4].

High energy mechanical ball milling has been used as an alternative method, with the purposes to reduce the particle size in several materials, such as ferroelectrics and magnetics, and to increase the sinterability of the calcinated powders [1,13–16]. This process takes place at room temperature in well sealed containers, avoiding loss and volatilization of the components.

On the other hand, nanostructured materials have received a lot of attention during the last decade; mainly due to their novel properties [17–19]. In order to obtain nanostructurated ceramics during the sintering process, it is important that the grain size used be lower than 100 nm. Several sintering methods have been used to obtain nanostructurated ceramics; among then, the fast firing [20–23] and spark plasma [24,25] have been widely used. It is well-known that the fast firing process of pressed powders provides higher densities than conventional sintering processes. This process has been successfully used in the sintering of some materials, such us: $BaTiO_3$, $PbZr_{0.52}Ti_{0.48}O_3$, $PbMg_{1/3}Nb_{2/3}O_3$, etc, resulting in high-quality ceramics [26–28].

In this work we report the preparation of $PbZr_{0.6}Ti_{0.4}O_3$ nanopowders and nanostructured ferroelectric ceramics by ball milling process and fast firing methods, respectively. Moreover, the influence of the milling time on the nanoparticles size and the sintering parameters on the microstructure has been investigated, as well as their influence in the dielectric properties of the nanostructured ceramics.

2. Experimental procedure

Precursor calcinated powders with the nominal formula $PbZr_{0.6}Ti_{0.4}O_3$ were prepared by the solid-state reaction method. For this purpose, stoichiometric quantities of precursor oxides (lead oxide (PbO) and zirconium oxide (ZrO_2) 99.9% pure and titanium oxide (TiO_2) 99.7% pure supplied by Aldrich were mixed for 20 h in a ball milling container, containing isopropyl alcohol and stabilized by ZrO_2 cylinders. These oxide mixtures were calcinated at 850°C for 3.5 h based on thermogravimetry (TG) and differential thermal analysis (DTA) curves, which were carried out by a simultaneous thermogravimetric-differential scanning calorimetric Netzsch STA 409 EP type analyzer. At room temperature and normal air pressure conditions, the precursor $Pb(Zr_{0.6}Ti_{0.4})O_3$ calcinated powders were subjected to a high-energy ball milling operation by using a Reutech 2 planetary ball milling system. A 250-ml zirconium vial and balls with 3 mm of diameter and a powder weight ratio (BPR) of 15 ball/gram were used as milling container. This container was rotated at 400 rpm (milling speed) using different milling times (20, 40, 60 and 80 h). In order to avoid overheating, the milling system was turn off during 5 min after 60 min of running.

With the objective to get a complete characterization of the milled powders, their sintering behaviour was also monitored by a Netzsch 404 EP type dilatometer. PZT powders, resulting of 60 h of ball milling, were pressed into 10-mm diameter pellets and

sintered in air atmosphere by fast firing method. For this process, the pellets were directly introduced inside a furnace, previously heated at 950°C, and kept it there for 30, 45, 60, 90 and 120 min, resulting in the *so-called* S1, S2, S3, S4 and S5 samples, respectively. Afterwards, the samples were quenched at room temperature and post-annealed at 800°C for 4 h.

PZT powders with 3 wt.% of lead oxide excess, resulting in 60 h of ball milling, were also prepared under the above-mentioned conditions. This was carried out in order to compensate for the lead losses occurred during the fast firing sintering process and to increase the density of the samples. These samples were *called* S6, S7, S8, S9 and S10, respectively.

The PZT ceramics density was obtained by the well-known Archimedes method, while theoretical density was determined based on the lattice parameters and the samples molecular weight. X-ray diffraction (XRD) patterns were recorded by a Rigaku D-max diffractometer with copper k_α radiation. The measurements were performed in continuous mode from 10° to 80° in 2θ. Average crystallites size and lattice strain of the milled powders were estimated by peak broadening techniques.

Scanning electron microscopy plan-view images for milled powder were achieved by a Jeol 5400 LV electron microscope. The surface grain morphology of the samples was also analysed by atomic force microscopy (AFM) technique, using a Shimadzu WET-SPM 9600 microscope, working in contact mode.

The dielectric measurements were carried out by a HP-4194A impedance gain phase analyzer. These measurements were performed in heating and cooling modes at a constant rate of $2°C\,min^{-1}$ over a temperature range of 24°C up to 650°C.

3. Results and discussion

Figure 1 shows the XRD patterns of the unmilled and milled 850°C calcinated powders. XRD peaks observed in these powders belong to a pure PZT phase, according to the JCPDS datafile N° 33-784. Moreover, no significant changes are observed in the intensity of the main diffraction peaks, while the increase of the wideness of the milled PZT powder

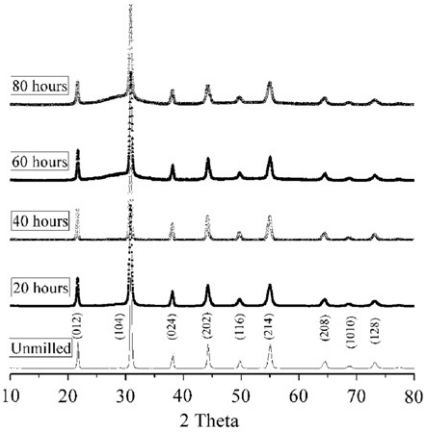

Figure 1. XRD patterns of $PbZr_{0.6}Ti_{0.4}O_3$ calcined powders, unmilled and milled during 20, 40, 60, and 80 h to 400 rpm and BPR = 15 in air at room temperature.

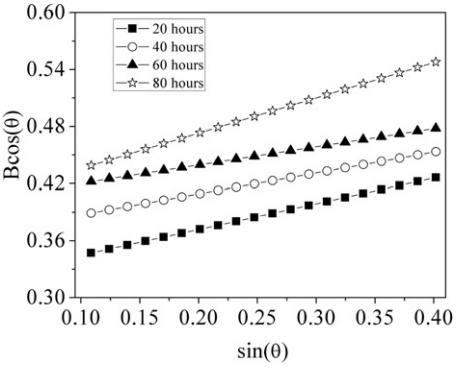

Figure 2. B cos θ is plotted against sin θ for the milled sample at 400 rpm during 20, 40, 60 h and 80 h and BPR = 15.

diffraction peaks is associated to the decrease of the particle size after the calcinated powder milling process.

Crystallite size of the powder particles and their lattice strain were determined by X-ray peak broadening techniques, using the following equation [19].

$$B = \frac{0.9\lambda}{d\cos\theta} + \eta\tan\theta \tag{1}$$

where η is the lattice strain, d the crystallite size, λ the wavelength of the incident X-ray radiation, B the full width at half maximum (FWHM) intensity of the peak and θ the Bragg angle. After a simple mathematical re-arrange the Equation (1) can be written as

$$B\cos\theta = \frac{0.9\lambda}{d} + \eta\sin\theta \tag{2}$$

Thus, it is convenient to plot the $B\cos\theta$ against $\sin\theta$ with the purpose to obtain the slope (η) and the intercept (0.9 λ /d) of the straight line. Based on these results, we can calculate the crystallite size (d) and the lattice strain (η) of the milled 850°C calcinated powders, as shown in Figure 2.

Figures 3 and 4 show the milling time dependence of the d and η parameters, respectively. The crystallite size decreases with an increase of the milling time, reaching saturation near to 40 h. On the other hand, the lattice strain also decreases with the increase of the milling time; however, after the 60 h it increases, probably due to the increase of structural defects in the crystalline lattice [19]. Similar analyses have been carried out on other materials, under the same milling conditions, resulting also in a significant reduction of the crystallite size [12,29].

There is not a well-established theory to explain the above-mentioned phenomena. However, it has been accepted that during the high-energy milling process there are three main milling stages: particle refinement, particle size homogenization and particle structure defect formation. In the early hours of the milling process, the 850°C calcinated PZT powders are greatly refined, both particle and crystallite size (first stage), being followed by a visible degree of the particle size homogenization (second stage). Finally, in the latest hours (last stage), the milling is mainly focused on the PZT powders, resulting in an increase of the structural defects and disorder of the milled powders. It has already been observed that the increase of defect and disorder by the milling process enhanced the sinterability and increase the lattice strain of the PZT powders [19].

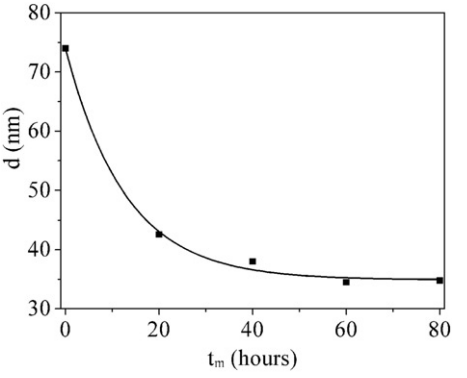

Figure 3. Milling time dependence of the crystallite size for the unmilled and 20, 40, 60 and 80 hours milled samples.

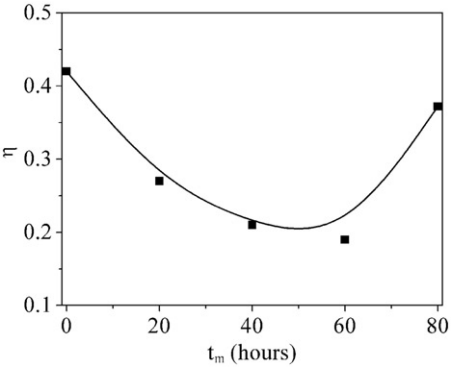

Figure 4. Milling time dependence of the strain for the unmilled and 20, 40, 60 and 80 hours milled samples.

Figure 5(a), 5(b) and 5(c) show the scanning electron microscope (SEM) images of the calcinated powders milled for 20, 40 and 60 h, respectively. In all the images powder agglomerates are observed, which decrease in size as the milling time increases. These agglomerates are compacts with a sized distribution from 1–10 μm; however, small individual particles are also observed with a size of ~100 nm.

Figure 6(a) and 6(b) show the TG and DTA curves carried out on unmilled and milled calcinated powders. In Figure 6a, a thermal decomposition stage is observed from room temperature up to ~320°C. It is practically inexistent in unmilled powders but clearly observed in milled powders, increasing with the increase of milling time. The higher effective surface as the particle size decreases with the milling time is responsible for this effect. The higher electrostatic interaction between the particle effective surface area and the environmental water results in a higher water absorber powder, which is eliminated during the first heating stage (25–320°C). The weight losses remain practically constant from 320°C up to 1000°C (second stage). Finally, above the 1000°C mark, the weight losses increase drastically, which is clearly associated with the lead volatilization. A shift to lower temperatures in the lead volatilization process is also observed as the number of hours of PZT powder ball milling increase.

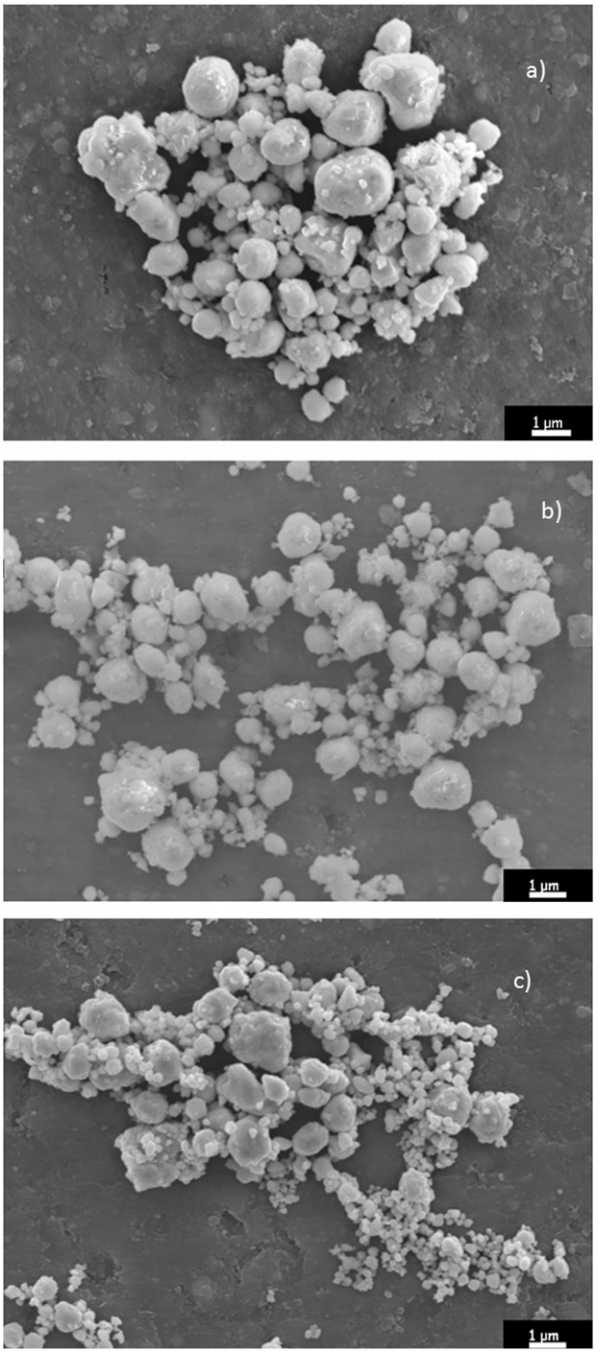

Figure 5. SEM images of (a) 20 hours, (b) 40 hours and (c) 60 hours milled PZT powders.

DTA curves are in correlation with the TG analysis, showing that lead volatilization starts to take place at temperatures relatively lower than the reported in the TG analysis (~1000°C). Moreover, DTA analysis also show that the starting lead volatilization temperature is a function of the milling time, shifting from 850°C in unmilled powder up to

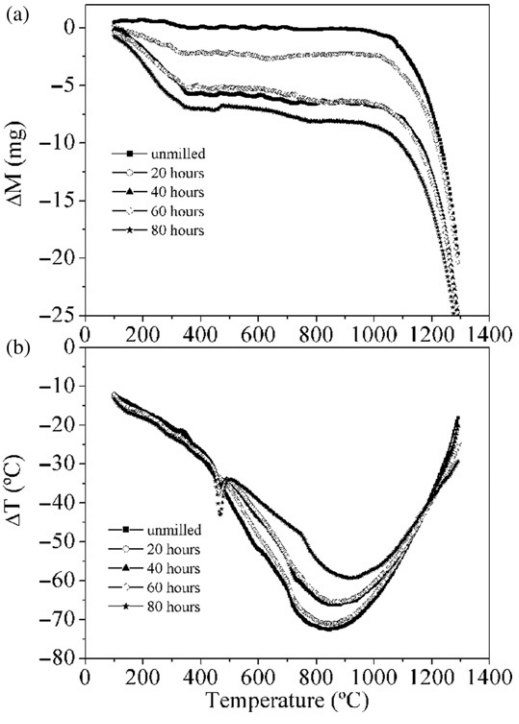

Figure 6. TG and DTA curves of the unmilled and milled PZT powders at 400 rpm during 20, 40, 60 and 80 hours.

930°C in 80 h milled powders and that the thermal energy needed to obtain the PZT phase (ΔT) is also a function of the ball milling time, decreasing as the milling time increases. There is a DTA anomaly at 460°C, which result in a narrow exothermic peak for powders milled during a long period of time (60 and 80 h). This modification in the 460°C exothermic peak might be associated to structural changes, because weight losses are not observed at this temperature (i.e. a ferroelectric-paraelectric phase transition). The decrease of the particle size, and in consequence the increase of the structural freedom of the particle, could be the responsible of this narrow peak apparition in the DTA curves.

Figure 7 shows the temperature dependence of the linear sintering rate for the 850°C calcined powder, milled at 20, 40, 60 and 80 h. The linear sintering rate curves reveal two densification peaks, which are associated with the sample shrinkages occurred in the 650–1050°C temperature range. The first densification maximum take place at ~780°C and it is attributed to a PbO-rich liquid phase formation, resulting from the relative low lead oxide melting point [20]. In this sintering stage, the main densification mechanism is associated with the particle rearrangement under the presence of the PbO-rich liquid phase. The result obtained is in good agreement with the reported by Hammer and co-workers for PZT and PLZT ceramics prepared by the conventional mixed-oxide process [20].

A second densification rate maximum is observed at 825°C and 805°C for 20 h and 40, 60 and 80 h milled powders, respectively, which is somehow associated with the different degrees of refinement and homogeneity of the milled powders. It is well-known that the

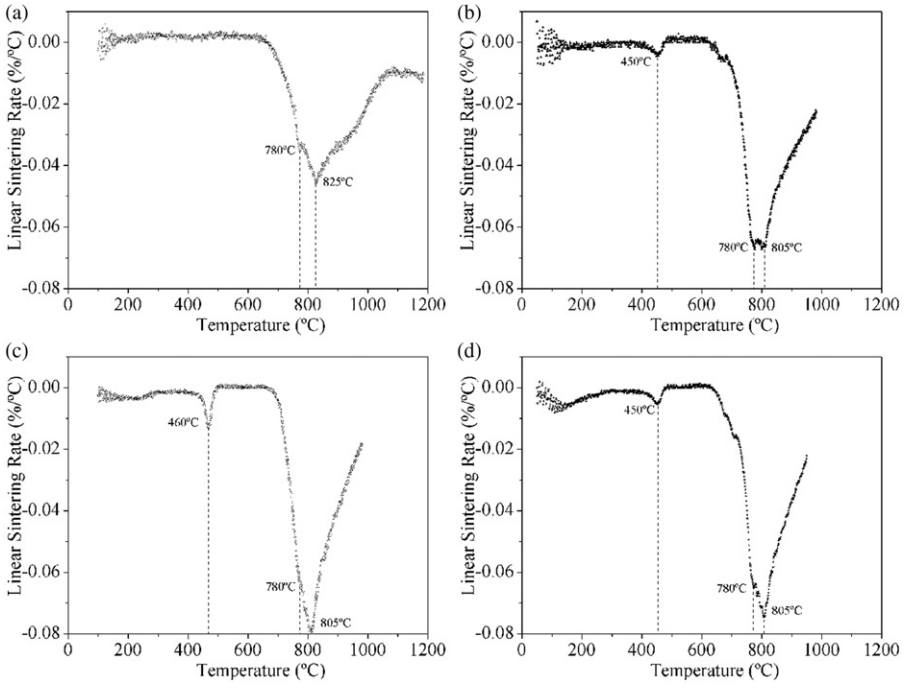

Figure 7. Sintering behavior of the (a) 20 hours (b) 40 hours (c) 60 hours and (d) 80 hours milled PZT powders.

second densification rate peak predicts the intermediate and final high temperature sintering stages of PZT powders prepared by a conventional mixed-oxide process under volume diffusion densification mechanism, which usually take place at ~1100°C [20]. However, in our samples this second maximum sintering rate takes place ~300°C lower than those reported for PZT powders prepared by conventional methods, clearly being associated with the ball milled process used. The above-mentioned confirm the applicability of the high-energy ball milling process for the preparation of PZT ceramics at lower temperatures.

After the linear sintering rate analysis the stoichiometric 60 h milled PZT powders were pressed into 10-mm diameter pellets and sintered at 950°C by fast firing method for 30 (S1), 45 (S2), 60 (S3), 90 (S4) and 120 min (S5). Table 1 shows shrinkage percent, weight losses and density of these samples. There is a slight increase of the volume shrinkage from 30 to 45 min in the sintering time. Afterward, it remains practically constant up to 90 min, increasing again at 120 min of sintering time. The weight losses show a similar behaviour than the volume shrinkage, except at 120 min of sintering time where it remains constant. There is no visible improvement in the bulk density of the PZT ceramics as the sintering time increases. Indeed, the density of the samples ($\rho \sim 91\%$) is too low to be considered as high quality ceramics ($\rho > 95\%$). It is evident that the increase in the rapid thermal annealed sintering time does not improve the quality of the 60 h milled PZT stoichiometric samples, probably due to the lead evaporation from the surface of the sample during the 950°C temperature sintering.

Table 2 shows shrinkage percent, weight losses and density of the 60 h milled PZT powders with 3% of PbO excess, pressed into 10-mm diameter pellets and sintered at

Table 1. Physical properties and sintering parameters of stoichiometric PZT sintered samples.

Parameters Samples	Volume shrinkage (%)	Weight losses (%)	Relative density (%)
S1	23.66	1.08	90.70
S2	25.96	1.58	91.6
S3	26.40	1.60	91.1
S4	26.41	1.69	91.9
S5	29.39	1.68	91.7

Table 2. Physical properties and sintering parameters of PZT sintered samples with 3% of lead excess.

Parameters Samples	Volume shrinkage (%)	Weight losses (%)	Relative density (%)
S6	26.24	1.85	95.7
S7	27.10	2.40	96.2
S8	27.98	2.71	97.4
S9	27.61	2.73	97.9
S10	27.85	2.78	97.7

950°C by fast firing method for 30 (S6), 45 (S7), 60 (S8), 90 (S9) and 120 min (S10). There is an increase of the shrinkage percent and weight losses for the lower sintering time periods, remaining practically constant after 45 min. Shrinkage percent, weight losses and density trends look similar to the observed in stoichiometric samples; however, the density of the samples is higher. It is clear that the 3% lead excess help the densification in liquid phase, avoid the lead defects in the structure and improve the densification of the samples. In this type of samples the lead oxide excess melts forming an abundant liquid phase, in contrast to stoichiometric samples where a less amount of liquid is formed; part of this liquid phase flows inside the solid solution compensating the lead defect and the rest is volatilized. The liquid phase formed during the sintering process at 950°C produces enough capillary pressure that allows large particle rearrangements in the samples [30].

On the other hand, squeezing out the lead oxide molten also gives rise to a lead compositional gradient in the sample; especially, in the surfaces of the pellets that become rich in PbO. In order to homogenize the samples, a post-sintering annealing treatment at a relative lower temperature (800°C) is carried out, which gives a uniform colour to the surface and interior of the samples. At the same time, the annealing treatment results in a controlled volatilization of lead oxide, achieving the desired sample composition.

Finally, the peak observed near to 450°C is associated with the ferro-paraelectric phase transition of the PZT system. This transition temperature is 70°C higher than that obtained by the dielectric measurements (shown below). However, this is not an incongruence result because the heating rates for both techniques ($10^{\circ}C\,min^{-1}$ in the dilatometric measurement and $2^{\circ}C\,min^{-1}$ in the dielectric measurement) and the

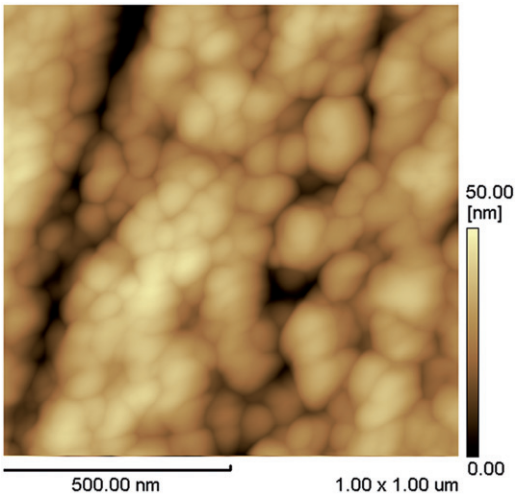

Figure 8. AFM topography image of the PZT (60/40) polycrystalline sample sintered by fast firing at 950°C during 60 min.

parameter involved in the measurements (structural change in the dilatometric measurement and intrinsic and extrinsic changes of the dielectric constant associated with the structural and polarization changes in the dielectric measurement) are different.

Figure 8 shows a representative AFM surface image of the PZT sintered samples prepared from 60 h milled powder with 3% of lead excess. This image shows a compact structure with grain sizes from 50 to 90 nm, representative for all the samples because the sintering time conditions practically do not modify the grain size of the samples.

Figure 9 shows the dielectric constant and dielectric losses temperature dependence (at several frequencies) for the S8 PZT ceramic. It is observed that there is no remarkable temperature shift in the dielectric constant maximum ($T_m = 375$°C) as the driving frequency increases. Moreover, over the ferroelectric-paraelectric transition temperature (T_m), the lower frequencies' (<100 kHz) dielectric permittivity responses increase, which is associated with low-frequency conductive processes [31].

The 1 MHz temperature dependence of the dielectric losses also shows the ferroelectric-paraelectric phase transition at 375°C (Figure 9b). However, at driving frequencies below 100 kHz, the dielectric and conductive losses are overlapped, mitigating the ferroelectric-paraelectric phase transition peaks. In the dielectric losses curves it is also observed that the low-frequency conductive processes begin to take place at temperatures near to 200°C.

4. Conclusions

Calcinated PZT (60/40) nanopowders were milled by high-energy ball milling technique. This process results in a decrease of the crystallite size in the first 40 h of milling and a constant crystallite size for higher milling time. Higher milling times also increase the defects and disorder, resulting in an enhanced sinterability of the PZT powders. On the other hand, TG and DTA of the unmilled and milled powders show an increase in the environmental water absorption, a decrease of the starting lead oxide volatilization temperature and reveal structural changes at 450°C as the milling time increases.

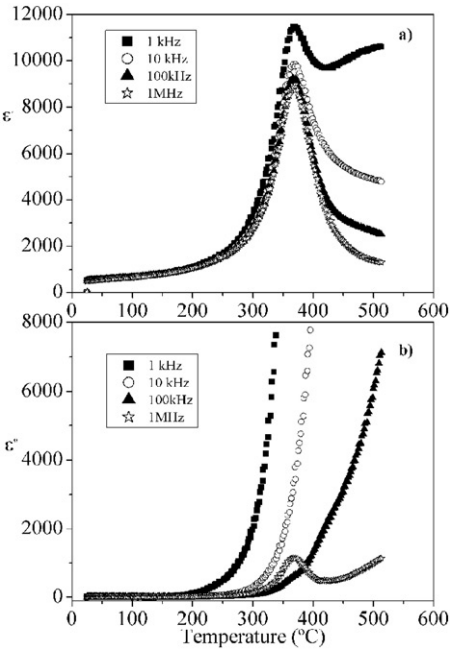

Figure 9. Temperature dependence of the dielectric constant and dielectric losses (at several frequencies) of PZT ceramics sintered by fast firing method at 950°C for 60 minutes.

Nanoestructured ceramics with grain sizes of 50–90 nm were obtained using the same fast firing sintering conditions (950°C/60 min and a post-sintering annealing treatment at 800°C/4 h, in the sample with an excess 3% PbO). The dielectric properties of the high-density S8 PZT sample reveal that high-energy ball milling and fast firing are effective techniques to prepare PZT nanoestructured ceramics at a relatively low-temperature (950°C).

Acknowledgements

The authors thank FAPES-Brazilian agency for financial support (Project No. 2008/04023-7). They also thank F.J. Picon for his technical assistance.

References

[1] J. Xue, J. Wang, and T. Weiseng, *Hydriding/dehydriding properties of nanocrystalline $Mg_{87}Ni_3Al_3M_7$ (M = Ti, Mn, Ce, La) alloys prepared by ball milling*, J. Alloy. Compd. 308 (2000), pp. 139–146.
[2] B. Jaffe, R. Cook Jr, and H. Jaffe, *Piezoelectric Ceramics*, Academic Press, New York, 1971.
[3] H. Haertling, *Ferroelectric ceramics: History and technology*, J. Am. Ceram. Soc. 82 (1999), pp. 797–818.
[4] E.L. Eskandarani and M. Sherif, *Mechanical Alloying for Fabrication of Advanced Engineering Materials*, Noyes Publications, New York, 2001.
[5] A.D. Romig Jr, M.T. Dugger, and P.J. McWhorter, *Materials issues in microelectromechanical devices: Science, engineering, manufacturability and reliability*, Acta Mater. 51 (2003), pp. 5837–5866.

[6] R.C. Buchanan, *Ceramic Materials for Electronics*, 2nd ed., Vol. 182, Marcel Dekker Inc., New York, 1991.
[7] G.H. Haertling and C.E. Land, *Recent improvements in the optical and electrooptic properties of PLZT ceramics*, Ferroelectrics 3 (1972), pp. 269–280.
[8] G.S. Snow, *Improvements in atmosphere sintering of transparent PLZT ceramics*, J. Am. Ceram. Soc. 56 (1973), pp. 479–480.
[9] D.M. Ibrahim and H.W. Hennicke, *Preparation of lead zirconate by a sol gel method*, Trans. J. Br. Ceram. Soc. 80 (1981), pp. 18–22.
[10] S. Sato, T. Murakata, H. Yanagi, F. Miyasaka, and S. Iwaya, *Hydrothermal synthesis of fine perovskite $PbTiO_3$ powders with a simple mode of size distribution*, J. Mater. Sci. 29 (1994), pp. 5657–5663.
[11] A. Wu, P.M. Vilarinho, I.M. Miranda Salvado, and J.L. Baptista, *Sol–gel preparation of lead zirconate titanate powders and ceramics: Effect of alkoxide stabilizers and lead precursors*, J. Am. Ceram. Soc. 83 (2000), pp. 1379–1385.
[12] B.G. Muralidharan, A. Sengupta, G.S. Rao, and D.C. Agrawal, *Powders of $Pb(Zr_xTi_{1-x})O_3$ by sol-gel coating of PbO*, J. Mater. Sci. 30 (1995), pp. 3231–3237.
[13] D.J. Fatemi, V.G. Harris, V.M. Broning, and J.P. Kirkland, *Processing and cation redistribution of MnZn ferrites via high-energy ball milling*, J. Appl. Phys. 83 (1998), pp. 6867–6869.
[14] X. Junmin, T. Yunling, W. Dongmei, and J. Wang, *Synthesizing 0.9PZN–0.1BT by mechanically activating mixed oxides*, Solid State Ionics 120 (1999), pp. 183–188.
[15] C. Gomez-Yañes, C. Benitez, and H. Balmori-Ramirez, *Mechanical activation of the synthesis reaction of $BaTiO_3$ from a mixture of $BaCO_3$ and TiO_2 powders*, Ceram Int. 26 (2000), pp. 271–277.
[16] L.B. Kong, W. Zhu, and O.K. Tan, *$PbTiO_3$ ceramics derived from high-energy ball milled nano-sized powders*, J. Mater. Sci. Lett. 19 (2000), pp. 1963–1966.
[17] H. Gleiter, *Materials with ultrafine microstructures: Retrospectives and perspectives*, Nanostruct. Mater. 1 (1992), pp. 1–19.
[18] R. Birringer, *Nanocristalline materials*, Mater. Sci. Eng. A-Struct. 117 (1989), pp. 33–43.
[19] C. Suryanarayana, *Mechanical alloying and milling*, Prog. Mater. Sci. 46 (2001), pp. 1–184.
[20] M. Hammer and M.J. Hoffmann, *Sintering model for mixed-oxide-derived lead zirconate titanate ceramics*, J. Am. Ceram. Soc. 81 (1998), pp. 3277–3284.
[21] C.E. Baumgartner, *Fast firing and conventional sintering of lead zirconate titanate ceramic*, J. Am. Ceram. Soc. 71 (1988), pp. C350–C353.
[22] A.W. Searcy, *Theory for sintering in temperature gradients: Role of long-range, mass transport*, J. Am. Ceram. Soc. 70 (1987), pp. C61–C62.
[23] S.S. Chiang, M. Nishioka, R.M. Fulrath, and JA. Pask, *Effects of processing on microstructure and properties of PZT ceramics*, Am. Ceram. Soc. Bull. 60 (1981), pp. 484–489.
[24] Y. Aman, V. Garnier, and E. Djurado, *Influence of green state processes on the sintering behaviour and the subsequent optical properties of spark plasma sintered alumina*, J. Eur. Ceram. Soc. 29 (2009), pp. 3363–3370.
[25] J. Liu, Z. Shen, M. Nygren, Y. Kan, and P. Wang, *SPS processing of bismuth-layer structured ferroelectric ceramics yielding highly textured microstructures*, J. Eur. Ceram. Soc. 26 (2006), pp. 3233–3239.
[26] J.W. Laughner, F.J. Calnan, B. Borglum, and L.M. Falter, *Centrifugation and fast firing of a commercial $BaTiO_3$ powder*, Sixth IEEE Int. Symp. on Appl. Ferroelectrics (1986), pp. 381–383.
[27] A. Seal, R. Mazumder, A. Sen, and H.S. Maiti, *Fast firing of lead zirconate titanate ceramics at low temperature*, Mater. Chem. Phys. 97 (2006), pp. 14–18.
[28] C. Miclea, C. Tanasoiu, C.F. Miclea, L. Amarande, R. Iorgulescu, V. Tanasoiu, and S. Moscu, *Advanced technology for making PZT type ceramics by fast firing*, J. Optoelectron. Adv. M. 3 (2001), pp. 83–87.

[29] R. Hansch, S. Seifert, W. Braue, D. Sporn, and G. Muller, *The effects of the PbO content upon the microstructure and the ferroelectric properties of undoped sol-gel derived PZT(53/47) fibers*, J. Eur. Ceram. Soc. 24 (2004), pp. 2485–2497.

[30] S. Begin-Colin, G. Le Caer, M. Zandona, E. Bouzy, and B. Malaman, *Influence of the nature of milling media on phase transformations induced by grinding in some oxides*, J. Alloy. Compd. 227 (1995), pp. 157–166.

[31] Y. Leyet, F. Guerrero, J. de los, S. Guerra, M. Venet, and J.A. Eiras, *Investigation of the dielectric response in $PbNb_2O_6$ ferroelectric ceramics*, J. Appl. Phys. 101 (2007), pp. 064105–064109.